NK-Cell-Encapsulated Porous Microspheres via Microfluidic Electrospray for Tumor Immunotherapy

Dan Wu, Yunru Yu, Cheng Zhao, Xin Shou, Yun Piao, Xin Zhao*, Yuanjin Zhao*, and Shuqi Wang*

Abstract

Immunotherapy has recently garnered significant research interest in the field of clinical cancer management. The potential of tumor immunotherapy has been demonstrated for targeting a variety of tumors, both in vivo and in vitro, yielding some remarkable therapeutic effects. Herein, inspired by the stem cell niche, we developed a scale-up approach to generating porous microspheres with encapsulated natural killer (NK) cells via microfluidic electrospray for in situ tumor immunotherapy. The generated microspheres contained porous microstructures with tunable morphologies because of versatile but precise fluid control in the microfluidic electrospray system. NK-92MI cells encapsulated in porous microspheres were protected from the outer complex environment, allowing for improved proliferation and functionality. As observed, perforin and granzymes were sustainably secreted from the encapsulated NK-92MI cells, which exhibited robust killing effects on tumors both in vitro and in vivo. With continual proliferation, NK-92MI cells budded from the surface of porous microspheres and migrated into the surrounding residual tumor tissues, further destroying tumor cells. More importantly, no side effects owing to the native host immune system were observed by injecting the NK-92MI cell-encapsulated microspheres into tumors in vivo. Therefore, the NK-cell-encapsulated porous microspheres show great potential for tumor immunotherapy, offering a robust and attractive treatment option for cancer patient management

KEYWORDS: microfluidics immunotherapy natural killer cell hydrogel tumor

Introduction

As cancer is a worldwide problem that seriously affects human health, several standard treatment strategies such as surgical resection, radiotherapy, chemotherapy, and immunotherapy have been developed. (1) Among these strategies, cancer immunotherapy, which is based on the ability of immune cells to recognize and attack tumor cells, has been recognized as one of the most effective treatment options. (2,3) The development of tumor immunotherapy has several development stages ranging from cytokine therapy to engineered immunotherapy. Cytokine therapy involves injecting large doses of cytokines into the vein of the patients and activating the patients' lymphocytes to kill tumor cells. (4−6) Although this treatment strategy has benefited the management of specific types of malignancies, large doses of cytokines can cause serious side effects. (7−9) In addition, the complex tumor microenvironment renders it difficult to achieve desired and efficient therapeutic effects by injecting cytokines alone. (10) Alternatively, adoptive therapies based on immune cells (11) such as cytokine-induced killer (CIK) cells, (12) chimeric antigen receptor T-cell immunotherapy, (13) natural killer (NK) cells, (14) etc. have gradually emerged. These immune

cells are activated or modified in vitro and then intravenously injected into the patient's body through blood circulation to kill tumor cells. Compared with CIK and T lymphocytes, NK cells can directly kill tumor cells without the requirement for prior sensitization via antigens presented by dendritic cells. Currently, tumor immunotherapies based on the infusion of autologous and allogeneic NK cells have been extensively evaluated in phase 1 or phase 2 clinical trials, which have reported some encouraging clinical outcomes. (15−18) Despite the successes in cell-based tumor immunotherapy, immune cells still possess severe off-target effects by attacking normal tissues and organs due to their nonspecificity. (19−22) Also, excessive cytokines can be produced in cell-based tumor immunotherapy, which can in turn induce severe side effects like cytokine storms (9) and pose a great threat to patients' health. Therefore, novel immunological anticancer therapies with curative potentials and minimal side effects are yet to be developed.

In this paper, inspired by the microstructure of stem cell niche, (23) we produced porous microspheres on a large scale via microfluidic electrospray and encapsulated them with NK cells for tumor immunotherapy, as schemed in Figure 1. Microfluidic electrospray is an advanced technology for precisely operating small volumes of fluids, and it can enhance the generation of monodisperse droplets with complex structures and compartments. (24−27) These droplets have been used as a means to fabricate functional microcarriers with cell encapsulation for a variety of applications. (28−34) However, the encapsulation of NK cells in porous microspheres for anticancer immunotherapy has not yet been investigated.

Figure 1

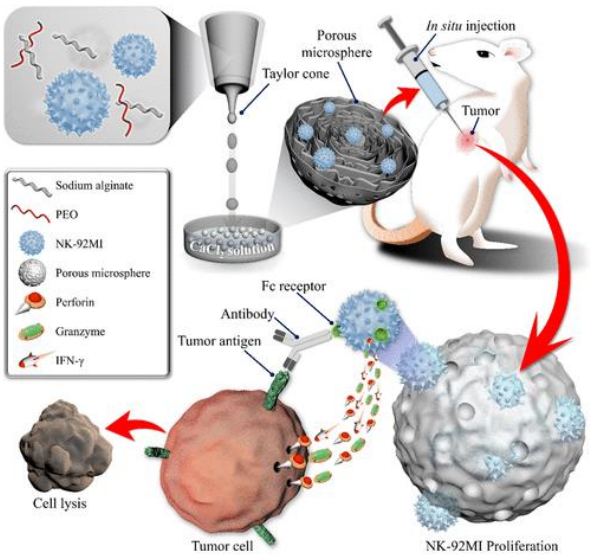

Figure 1. Schematic diagram of the fabrication and *in situ* injection of NK-92MI-laden poly (ethylene oxide) (PEO)/alginate solution (ALG) porous microspheres for tumor immunotherapy.

We herein used a simple microfluidic electrospray method to encapsulate NK-92MI cells into porous hydrogel microspheres for in situ injection into tumors. Because the microspheres possess good permeability and allow rapid exchange of nutrients, the encapsulated NK-92MI cells proliferated and functioned well in this system. It was found that in their early stage, the NK-92MI cell-loaded microspheres could destroy tumor cells by secreting perforin, granzymes, etc. Furthermore, the tumor-killing effect of the NK-92MI cell-encapsulated microspheres was enhanced due to the budding of NK-92MI cells from the outer surface of the microspheres,

leading to the direct interaction with surrounding tumor tissues. Of note, the porous hydrogel microspheres can potentially protect the encapsulated NK-92MI cells from modulation of the tumor microenvironment and the rejection from the host's immune system. These features enable the application of porous microspheres encapsulated with NK cells for current clinical research and open up a new realm for anticancer immunotherapy.

Results and Discussion

Generation of Porous Microspheres via Microfluidic Electrospray

In a typical experiment, alginate solution (ALG) mixed with poly (ethylene oxide) (PEO) was used as the precursor solution for the generation of porous microspheres. During the electrospray process, the precursor solution was injected through a simple microfluidic device. Under the electric field created by a high voltage direct current instrument, the precursor solution was driven to form a "Taylor cone" at the outlet and turned into droplets while falling (Figure 2A). The droplets were then rapidly solidified in calcium chloride (CaCl2) solution. Based on the electrospray microfluidic technology, monodisperse and nearly spherical microspheres were obtained with diameters ranging from 250 to 700 μm (Figure 2B–D). By applying different parameters, microspheres with four different size distributions were formed and analyzed (Figure 2E–G). Compared with the alginate microspheres, the generated PEO/ALG microspheres had a greater number of pores because the PEO did not react with the calcium ions and would be removed after washing, leaving pores inside the microspheres. The improved porosity could endow the microspheres with enhanced oxygen and nutrient exchange efficiency, increasing cell survival and promoting cell proliferation. It should be mentioned that the microspheres with various diameters can be obtained by adjusting different parameters including voltage, diameter of the tip, flow rate, and the concentration of solutions. The diameter decreased from 2000 to 250 μm with an increasing electric voltage from 3 to 10 kV, as shown in Figure S1A. When the voltage reached 8 kV, the point of critical voltage was reached; newly created droplets were strongly pulled by the force of electric field and then were dispensed into the CaCl2 solution to form microspheres. At this stage, the diameters of the microspheres were only influenced by the diameter of the tip, the concentration, and the flow rate of solutions. Our results showed that the diameter of the microspheres increased from 250 to 550 μm as the diameter of the tip increased (Figure S1B). Additionally, microspheres with diameters ranging from 230 to 700 μm were observed by increasing the concentration or flow rate of the precursor solution (Figure S1C,D).

Figure 2

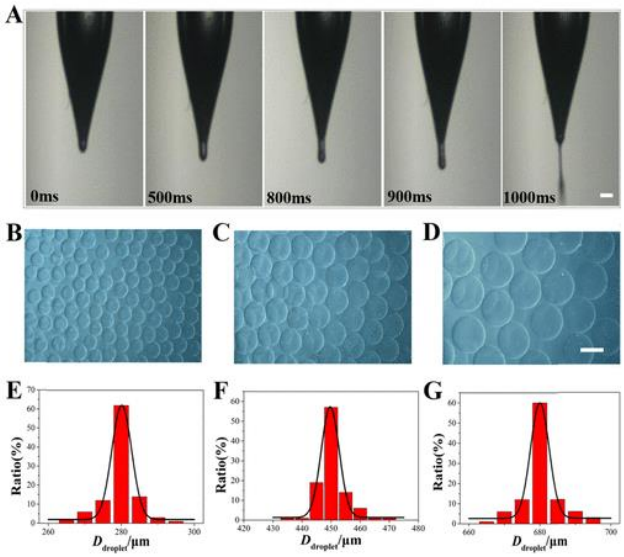

Figure 2. Generation of PEO/ALG microspheres via microfluidic electrospray. (A) The formation of PEO/ALG droplets during the process of microfluidic electrospray. Scale bar is 200 μm. (B–D) Bright-field microscopic images of PEO/ALG porous microspheres. Scale bar is 500 μm. (E–G) Diameter distribution of PEO/ALG porous microspheres, 100 microspheres were measured for each map.

Functional Characterization of the NK-92MI Microspheres

The resultant porous microspheres were subsequently used to encapsulate NK-92MI cells for tumor immunotherapy. As the cell survival and proliferation play an essential role in the strength of tumor immunotherapy, the cell viability of NK-92MI cells incubated with porous microspheres was first measured. As shown in Figure S2, the cell viability was more than 85% even after 72 h of incubation, suggesting that porous microspheres were biocompatible with the NK-92MI cells. Next, NK-92MI-laden porous microspheres prepared via microfluidic electrospray were cultured in cell medium to test whether they were suitable for cell proliferation (Figure 3A). The results demonstrated that the NK-92MI cells proliferated well in the porous microspheres. When the culture continued, a large portion of proliferating NK-92MI cells began to bud from the surface of porous microspheres and resided in the periphery of the microspheres, allowing for increased tumor-killing capability. The viability of NK-92MI cells within 14 days was analyzed in Figure S3, demonstrating the applicability of porous microspheres for long-term culture of NK-92MI cells. The increased percentage of living cells revealed that the biocompatible microenvironment of the porous microspheres could protect and support the growth of NK-92MI cells. To study the therapeutic capability of these NK-92MI microspheres, the levels of NK-92MI-secreted cytotoxic factors such as interferon-γ (IFN-γ), granzyme B, and perforin in culture medium were measured (Figure 3B–D). The results showed that the level of IFN-γ, granzyme B, and perforin increased in the supernatant because of the continuous proliferation and secretion of NK-92MI cells, further indicating their potential for enhanced tumor killing.

Figure 3

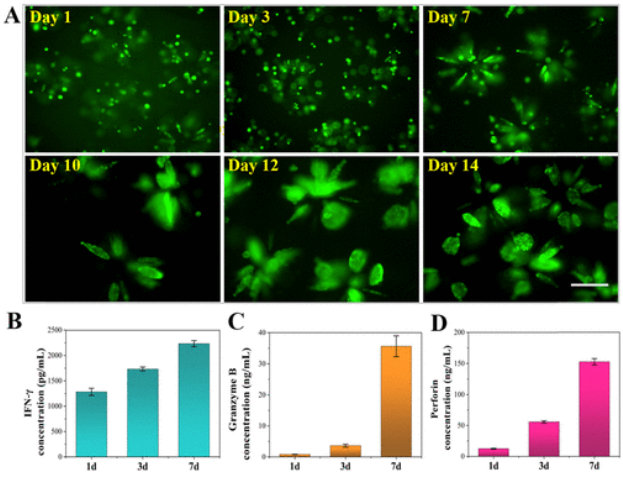

Figure 3. Proliferation of NK-92MI encapsulated in porous microspheres. (A) Representative images of NK-92MI cells in porous microspheres at day 1, 3, 7, 10, 12, and 14. Scale bar is 200 μm. (B–D) The secretion ability of NK-92MI microspheres at day 1, 3, and 7. IFN-γ, granzyme B, and perforin were measured using enzyme-linked immunosorbent assay (ELISA) kits according to the manufacturers' instructions.

In Vitro Tumor-Killing Effect of NK-92MI Microspheres

The killing capability of NK-92MI encapsulation microspheres can be attributed to the release of perforin and granzymes upon recognition and targeting of tumor cells through its activating receptors. Thus, the expression level of surface-activating receptors such as NKp30, NKp44, NKp46, and NKG2D was first characterized by flow cytometry (Figure S4A). The results showed that the NK-92MI cells highly expressed activating receptors of NKp30, NKp44, NKp46, and NKG2D, suggesting that the NK-92MI cells were highly activated and could directly kill tumor cells. The level of IFN-γ, perforin, and granzyme B secreted by NK-92MI cells was also confirmed using ELISA before they were encapsulated in porous microcapsules (Figure S4B–D). The results demonstrated that the NK-92MI cells secreted high levels of IFN-γ, perforin, and granzyme B and indicated that NK-92MI cells had the capability of sustainably secreting these tumor-killing factors. To prove this hypothesis, NK-92MI cells were then separately incubated with human breast cancer cells (i.e., MDA-MB-231) or human skin cancer cells (i.e., A375) for 4 h. Compared with the control group, live/dead staining showed that the NK-92MI killed 80% of tumor cells with an effector-to-target (E/T) ratio of 5:1. Among these groups, NK-92MI cells were more sensitive to A375 cells and had a relatively stronger killing effect. The tumor-killing efficiency was 90% with an E/T ratio of 1:1 (Figure S5A). The cytotoxic effects of the NK-92MI cells on MDA-MB-231 and A375 cells were also measured using the CCK8 assay. The results showed that the viability of MDA-MB-231 and A375 cells were significantly decreased after co-culturing with NK-92MI cells (Figure S5B,C). The cytotoxic activity of NK-92MI was also evaluated by detecting the level of lactic dehydrogenase (LDH) released from apoptotic tumor cells in the supernatant (Figure S5D), which also demonstrated that the NK-92MI had significant killing effects on MDA-MB-231 and A375 cells.

The tumor-killing effect of NK-92MI porous microspheres with E/T ratios of 1:1 and 5:1 was investigated (Figure S6). The NK-92MI microspheres were cultured with MDA-MB-231 or A375 cells for 6 h. Early apoptosis of tumor cells was observed after 6 h of coculture by

detecting Annexin V and propidium iodide (PI) using flow cytometry (Figure 4A). The apoptotic ratios of the MDA-MB-231 cells were 10.4 and 22.9% with E/T ratios of 1:1 and 5:1, respectively; Similarly, 19.9 and 28.9% of A375 cells apoptosed with E/T ratios of 1:1 and 5:1, respectively. These data showed that the NK-92MI microspheres had more killing effects on A375 cells. With longer co-culturing time for 24 h, the NK-92MI microspheres had significantly increased killing effects on tumor cells. The results showed that 80% of the MDA-MB-231 or nearly 100% of A375 cells were killed by NK-92MI microspheres with an E/T ratio of 5:1 (Figure 4B). This could be attributed to the proliferation of NK-92MI cells in porous microspheres with enhanced cellular functionalities. Therefore, the NK-92MI microspheres had a significantly elevated in vitro anticancer capability.

Figure 4

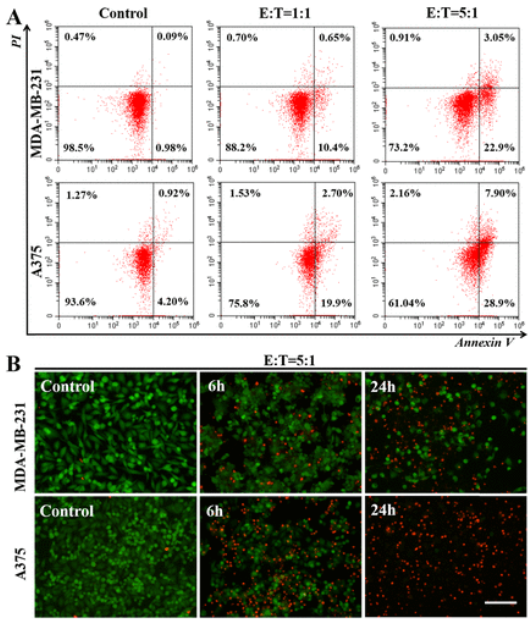

Figure 4. *In vitro* tumor-killing effect of NK-92MI microspheres. (A) Flow cytometry characterization of early apoptosis of MDA-MB-231 or A375 cells co-cultured with the NK-92MI microspheres for 6 h. (B) Live/Dead staining images of the NK-92MI microspheres against MDA-MB-231 and A375. Scale bar = 200 μm.

In Vivo Antitumor Therapy Efficiency of the NK-92MI Microspheres

The therapeutic effect of the NK-92MI microspheres was also investigated by in situ injection of nude mice with skin cancer (Figure 5A). An A375-bearing nude mice model was first established and in situ injected with NK-92MI microspheres around the tumor to evaluate the tumor-killing effect. An equal volume of 0.9% sodium chloride solution (NaCl) was injected as the control group. All of the mice were euthanized, and tumor samples were collected 14 days following the treatment. As observed in Figure 5B, tumors grew rapidly in the control group and the ALG microsphere group, while growing slowly in both the NK-92MI microsphere group and the NK-92MI group. Comparatively, the size of tumors in the NK-92MI microsphere group was smaller than that in the NK-92MI group. The average tumor volumes were analyzed, and they showed consistent results, indicating that the NK-92MI microsphere group had a stronger killing effect on tumor cells with long-term inhibition (Figure S7A). The body weight of the mice treated with the NK-92MI microspheres and the NK-92MI cells only had no significant decrease compared to the control group, indicative of the nontoxicity of the NK-

92MI-based tumor immunotherapy (Figure S7B).

Figure 5

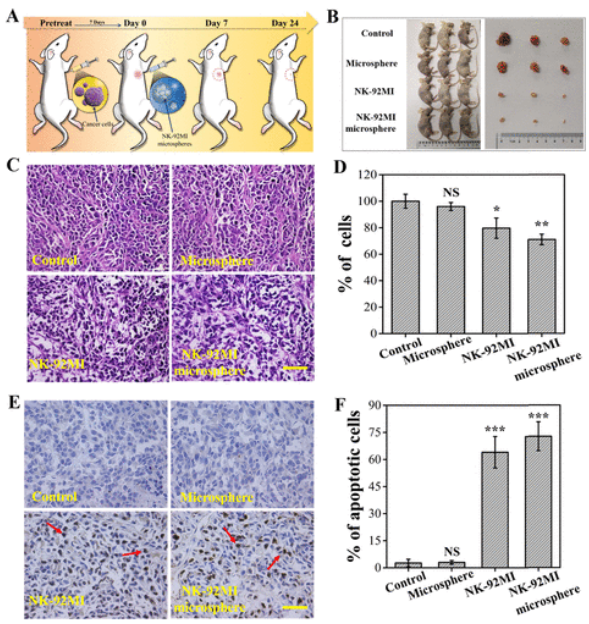

Figure 5. *In vivo* antitumor efficiency of NK-92MI microspheres. (A) The flow chart of the NK-92MI microspheres for *in situ* injection into A375-bearing mice. (B) Representative images of the mice with different treatments and the size of their respective tumor tissues as indicated. (C) Hematoxylin and eosin (H&E) stained images of tumor tissues after various treatments. (D) The percentage of tumor cells as indicated by the H&E assay (*$p < 0.05$, **$p < 0.01$). (E) Characterization of tumor tissues via immunohistochemical staining and terminal deoxynucleotidyl transferase dUTP nick end labeling (TUNEL) apoptosis analysis. The positive staining was indicated by red arrows. (F) Quantification of the expression of TUNEL assay (***$p < 0.001$). Scale bar = 50 μm.

To evaluate the therapeutic effect of the NK-92MI microspheres, pathological changes of tumor tissues were analyzed via hematoxylin and eosin (H&E) staining. In the control group and ALG microsphere group, the tumor cells were larger and densely populated, with more mitotic activity and less necrotic tumor cells. In contrast, the NK-92MI microsphere group and the NK-92MI group resulted in a smaller tumor cell mass with less mitotic activity and more necrotic tumor cells. Quantitative analysis exhibited that the percentage of tumor cells in the NK-92MI microsphere group was a little less than the NK-92MI group. These results suggested that the NK-92MI microsphere group slightly possesses higher therapeutic effects than the NK-92MI group (Figure 5C,D). Furthermore, terminal deoxynucleotidyl transferase dUTP nick end labeling (TUNEL) staining was used to assess the rate of apoptotic cells within tumor tissues obtained from each group. The apoptosis of tumor cells was observed in the NK-92MI microsphere group with a rate of approximately 75%. In contrast, there was no significant apoptosis in the control group and the ALG microsphere group (Figure 5E,F). Proliferation-associated nuclear antigen (Ki67) and proliferating cell nuclear antigen (PCNA) are indicators of tumor proliferation and are highly correlated with tumor progression. Thus, the expression of Ki67 and PCNA within tumor tissues was detected by immunohistochemistry (IHC). The results showed that both Ki67 and PCNA in the NK-92MI microsphere group and the NK-92MI group were less significantly expressed than that in the control group and ALG microsphere group (Figure 6A). Among all of the groups, the NK-92MI microsphere group had the lowest expression of PCNA and Ki67 in tumor tissues with a positive rate of approximately 20 and

10%, respectively. As CD31 is closely related to the angiogenic ability of tumors, the level of CD31 expression in the tumor tissues was also evaluated. Similarly, the expression of CD31 in tumor tissues in the NK-92MI microsphere group and NK-92MI group was significantly lower than that in the control group and the ALG microsphere group. Furthermore, the expression of CD31 in the NK-92MI microsphere group was less than that in the NK-92MI group, indicating that the NK-92MI microspheres had stronger inhibition of tumor angiogenesis and prevented tumor growth (Figure 6A). Quantitative analysis of PCNA, Ki67, and CD31 expression demonstrated that there were significant differences between the NK-92MI microsphere group and the other groups (Figure 6B–D). Those results confirmed that the NK-92MI microspheres induced tumor cell apoptosis through secreted perforin and granzyme B, as well as direct killing of NK-92MI cells budding from the surface of the microspheres.

Figure 6

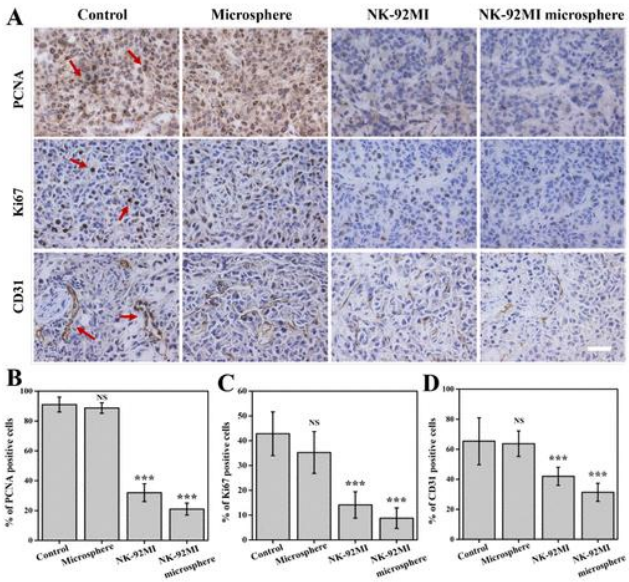

Figure 6. NK-92MI microspheres impaired tumor proliferation and angiogenesis. (A) The representative immunohistochemical photographs of PCNA, Ki67, and CD31 in the tumor tissues after various treatments. The positive staining was indicated by red arrows. (B) Measurement of the expression level of PCNA in tumor cells (***$p < 0.001$). (C) Measurement of the expression level of Ki67 in tumor cells (***$p < 0.001$). (D) Measurement of the expression level of CD31 in tumor cells (***$p < 0.001$). Scale bar = 50 μm.

Conclusions

In this study, we reported the generation of large-scale NK-92MI-encapsulated porous microspheres via microfluidic electrospray for in situ tumor immunotherapy. Through the microfluidic-based electrospray technique, microspheres were fabricated in a continuous and tunable way. The microspheres with porous structures provided a superior living and proliferating microenvironment for the NK-92MI cells due to their biocompatibility. Compared with free NK-92MI cells, the porous microspheres encapsulated with the NK-92MI cells maintained a significant killing effect, especially in the in vivo environment, owing to sustainable release of perforin and granzyme B. Attractively, the NK-92MI cells can bud from the surface of microspheres in vivo and enable direct killing of surrounding tumor cells. In addition to enhanced tumor-killing effects, porous microspheres encapsulated with the NK-92MI cells via in situ tumor injection can potentially avoid systemic side effects, which are

commonly observed in current adoptive immunotherapies. Therefore, the porous alginate microspheres encapsulated with NK-92MI cells have great potential for improving tumor immunotherapy in cancer patient management.

Experimental Section

Materials

Sodium alginate, poly(ethylene oxide) (PEO) (average Mw = 900 000 Da), dimethyl sulfoxide, calcium chloride, and phosphate-buffered saline (PBS) were purchased from Sigma-Aldrich. Dulbecco's modified Eagle's medium (DMEM), fetal bovine serum (FBS), penicillin/streptomycin (P/S), Trypsin–EDTA solution, and α-modified eagle medium (α-MEM) were purchased from Gibco (Grand Island, NY). The Live/Deadcell viability kit was obtained from Thermo Fisher Scientific (Waltham, MA). Cell counting kit-8 (CCK8) and cytotoxicity LDH assay kit-WST were obtained from Dojindo (Kumamoto, Japan). NK-92MI cells were gifts from Prof. He Huang (Zhejiang University School of Medicine). Human breast cancer cell line, i.e., MDA-MB-231, and human skin cancer cell line, i.e., A375, were purchased from the American Type Culture Collection (ATCC) (Manassas, VA) and cultured according to the recommended protocols. IFN-γ, perforin, and granzyme B ELISA kits were purchased from Neobioscience Technology Ltd (Shenzhen, China). PE-conjugated anti-NKp30 (IgG1, AF29-4D12), anti-NKp44 (IgG2b, 44.189), PE-Cyanine7-conjugated anti-NKG2D (IgG2b, 1D11), and anti-NKp46 (IgG1, 9E2) antibodies were obtained from eBioscience (San Diego). Fluorescein isothiocyanate (FITC)-conjugated anti-CD56 (IgG2b, NCAM16.2) and PE-conjugated anti-CD3 (IgG2b, HIT3a) antibodies were obtained from BD Biosciences (San Jose, CA). All of the antibodies used for immunostaining were used according to the respective manufacturers' instructions.

Porous Microsphere Preparation and Characterization

PEO/ALG porous microspheres were prepared via phase separation and emulsion/solvent evaporation. Typically, ALG (0.2 g) was dissolved in 10 mL of ddH2O and was then stirred at 37 °C for 2 h to ensure full dissolution. Next, a PEO solution (1.0%, wt) was added in a dropwise manner into the ALG solution with a volume ratio of 1:1, and the mixture was stirred at 40 °C with a spinning speed of 400 rpm for 8 h. Then, the resultant solution was dispensed by a microfluidic electrospray to generate a large quantity of microspheres. The diameter of the microspheres was adjusted by different parameters (e.g., voltage, tip diameter). The resultant microspheres were then immersed into a 2% CaCl2 solution for 1 h prior to collection with the aid of a sieve. Subsequently, the microspheres were washed with ddH2O three times before lyophilization.

Biocompatibility of Porous Microspheres

The viability of the NK-92MI cells within the porous microspheres was evaluated using a CCK8 assay. The cell-laden microspheres containing NK-92MI (1 × 105 cells/mL) were plated in a 96-microwell plate and cultured for 24, 48, and 72 h. Following the incubation, 10 μL of CCK8 working solution was added in the cell culture media and then incubated for 3 h at 37 °C. Then, the optical density (OD) value was measured using a plate reader (Synergy HTX) at 450 nm.

Preparation of Cell-Laden Porous Microspheres

The NK-92MI cells were grown in α-MEM supplemented with 0.1 mM of 2-mercaptoethanol, 0.02 mM of folic acid, 0.2 mM of inositol, 12.5% of horse serum, and 12.5% of FBS. MDA-MB-231 and A375 cells were cultured in DMEM containing 10% FBS and 100 U/mL P/S at 37 °C perfused with humidified CO2 (5%). The NK-92MI cells were cultured and mixed with PEO/ALG solution at 1 × 106/mL. The cell-laden mixture was then dispensed using a microfluidic electrospray system to generate cell-laden droplets. Next, the resultant droplets were immersed into a 2% CaCl2 solution for 2 min to generate cell-laden microspheres. Finally, the cell-laden microspheres were washed with cell culture medium three times and cultured for downstream analysis.

Enzyme-Linked Immunosorbent Assay (ELISA)

The NK-92MI cells (0.1, 0.3, 0.5, 1 M/mL) or NK-92MI cells (1 × 106/mL) encapsulated in the porous microspheres were plated in 24-well dishes and cultured for 7 days. The supernatant at day 1, day 3, and day 7 was collected, and the concentrations of soluble cytokines such as IFN-γ, perforin, and granzyme B released into the medium were measured using their respective ELISA kits according to the supplier's instructions (Neobioscience, Shenzhen, China).

Live/Dead Staining and in Vitro Cytotoxicity Assay

To measure the viability of proliferating NK-92MI cells in porous microspheres within 14 days, Live/dead staining was used. 2 μL of Calcein-AM and 2 μL of PI solutions were added to 1 mL of PBS to create a staining solution. The cell medium was removed, and 300 μL of the staining solution was added directly to the NK-92MI microspheres. After 20 min of incubation at 37 °C in darkness, the NK-92MI cells in microspheres were imaged under a fluorescence microscope (Carl Zeiss, Germany). To measure the cytotoxic activity of NK-92MI, MDA-MB-231 cells (2 × 105/mL) or A375 cells (2 × 105/mL) were placed on a 24-well plate for 12 h and co-cultured with the NK-92MI at various E/T ratios for 4 h. The cytotoxicity of MDA-MB-231 and A375 cells was measured by Calcein-AM and PI staining as described above. The proliferation of MDA-MB-231 and A375 cells was measured using a CCK8 assay. Briefly, NK-92MI cells were co-cultured with MDA-MB-231 or A375 cells at various E/T ratios. Following the incubation for 4 h, 10 μL of the CCK8 reagent and 90 μL of culture medium were added to cells for another 3 h for color development. The OD value was collected using a microplate reader at the wavelength of 450 nm.

Lactate Dehydrogenase (LDH) Release Assay

The LDH release assay was carried out using the cytotoxicity LDH assay following the manufacturer's instructions (Dojindo, Kumamoto, Japan). In brief, the NK-92MI effector cells were co-cultured for 4 h with target cells such as MDA-MB-231 and A375 (1 × 104) at effector-to-target (E/T) ratios of 10:1, 5:1, 3:1, and 1:1. The supernatants were collected for the measurement of LDH released from dead cells. To this end, the absorbance color development was measured at the wavelength of 490 nm.

Flow Cytometry Assay

To stain the NK-92MI cells, they were first washed two times in FACS buffer (PBS supplemented with 0.1% NaN3 and 0.1% bovine serum albumin (BSA)) and pelleted by centrifuging at 400 g for 5 min. Antibodies including PE-conjugated anti-NKp30, anti-NKp44, PE-Cyanine7-conjugated anti-NKG2D and anti-NKp46 were added in the dark at 4 °C for 60 min with concentrations as specified by the manufacturer (eBioscience, San Diego, USA).

Isotype-matched irrelevant monoclonal antibodies were used to define nonspecific staining. Flow cytometry was then conducted using the Beckman Coulter FC500 system. In addition, the NK-92MI microspheres were co-cultured for 6 and 24 h with target cells such as MDA-MB-231 and A375 at effector-to-target (E/T) ratios of 5:1 and 1:1. An Annexin-V-FITC apoptosis detection kit (BD Pharmingen) was utilized to measure the rate of cell apoptosis in MDA-MB-231 and A375 cells. To this end, MDA-MB-231 and A375 cells were stained using FITC-conjugated Annexin V or PI prior to characterization by flow cytometry. The data of cell apoptosis were collected using FACS Calibur (BD Biosciences) and then analyzed using CellQuest Pro software.

In Vivo Tumor-Killing Effect of the NK-92MI Microspheres

BALB/c-nude mice (Changzhou Cavens Laboratory Animal Ltd) were inoculated intradermally in a shaved flank with 2 × 106 of A375 cells. After 7 days, mice were given intratumoral injection once in a week for two weeks with the following treatments: (a) 0.9% NaCl; (b) microsphere; (c) NK-92MI cells; or (d) NK-92MI microspheres. All of the formulations were prepared freshly prior to the treatment. The body weight of mice and the volume of tumor tissues were measured 3 times a week. All animal experiments were performed according to the Guideline for the Care and Use of Laboratory Animals from the National Institutes of Health (USA) and were approved by the Animal Ethics Committee of Southeast University (NO. 20190108006).

H&E and IHC Staining

BALB/c-nude mice were sacrificed after 14 days of treatment. The tumor tissues were harvested and then embedded in an optimal cutting temperature (OCT) compound (Sakura Finetek Inc.). Frozen sections were cut at a thickness of 7 μm. Following deparaffinization and rehydration in sodium citrate buffer (pH = 6.0) at ambient temperature for 10 min, the sectioned tumor tissues were then heated in a microwave for 20 min for antigen retrieval. Then, the tumor sections were treated with H2O2 (3%) for 10 min, which was followed by BSA blocking (5% of goat serum) for 1 h at ambient temperature. Primary antibodies were then incubated with the tumor sections at 4 °C overnight. For IHC staining, the primary antibodies such as rat anti-mouse CD31 (BD bioscience), rabbit anti-mouse Ki67 (Abcam), and rabbit anti-mouse PCNA (Abcam) antibodies were used. After washing, the tumor sections were further stained using biotinylated streptavidin-HRP, 3,3′-diaminobenzidine, and hematoxylin counterstain. The tumor sections were then dehydrated via gradient alcohols to xylene and finally covered in Permount Mounting Medium under a cover slip. All images were taken under 200/400 magnification at eight different locations.

Statistical Analysis

All of the data were statistically analyzed using Origin 9.1 software wherever appropriate. The data from each group are presented as mean ± SD, and the comparison was made between the groups with the aid of a one-way analysis of variance test. A p-value of less than 0.05 was used to determine the statistical significance.

Acknowledgments

We acknowledge the support from the General Program from the National Natural Science Foundation of China (31871016), the National Key Research and Development Program (2016YFC1101302), and National Major Science and Technology Projects (2018ZX10732401-

003-007) from the Ministry of Science and Technology of China, the National Key Scientific Instrument and Equipment Development Projects (61827806) from the National Natural Science Foundation of China, and the Key Research and Development Program (2019C03029) from the Science and Technology Department of Zhejiang Province, as well as the start-up fund (1-ZE7S), central research fund (G-YBWS), and intra-faculty fund (1-ZVPC) from the Hong Kong Polytechnic University.

References

(1) Bray, F.; Ferlay, J.; Soerjomataram, I.; Siegel, R. L.; Torre, L. A.; Jemal, A. Global Cancer Statistics 2018: GLOBOCAN Estimates of Incidence and Mortality Worldwide for 36 Cancers in 185 Countries. Ca-Cancer J. Clin. 2018, 68, 394−424.

(2) Chiossone, L.; Dumas, P. Y.; Vienne, M.; Vivier, E. Natural Killer Cells and Other Innate Lymphoid Cells in Cancer. Nat. Rev. Immunol. 2018, 18, 671−688.

(3) Mellman, I.; Coukos, G.; Dranoff, G. Cancer Immunotherapy Comes of Age. Nature 2011, 480, 480−489.

(4) Bukowski, R. M. Cytokine Therapy for Metastatic Renal Cell Carcinoma. Semin. Urol. Oncol. 2001, 19, 148−154.

(5) Dranoff, G. Cytokines in Cancer Pathogenesis and Cancer Therapy. Nat. Rev. Cancer 2004, 4, 11−22.

(6) Rosenberg, S. A.; Lotze, M. T.; Yang, J. C.; Linehan, W. M.; Seipp, C.; Calabro, S.; Karp, S. E.; Sherry, R. M.; Steinberg, S.; White, D. E. Combination Therapy with Interleukin-2 and Alpha-interferon for the Treatment of Patients with Advanced Cancer. J. Clin. Oncol. 1989, 7, 1863−1874.

(7) Capuron, L.; Ravaud, A.; Dantzer, R. Early Depressive Symptoms in Cancer Patients Receiving Interleukin 2 and/or Interferon alfa-2b Therapy. J. Clin. Oncol. 2000, 18, 2143−2151.

(8) Racke, M. K.; Bonomo, A.; Scott, D. E.; Cannella, B.; Levine, A.; Raine, C. S.; Shevach, E. M.; Röcken, M. Cytokine-induced Immune Deviation as a Therapy for Inflammatory Autoimmune Disease. J. Exp. Med. 1994, 180, 1961−1966.

(9) Tisoncik, J. R.; Korth, M. J.; Simmons, C. P.; Farrar, J.; Martin, T. R.; Katze, M. G. Into the Eye of the Cytokine Storm. Microbiol.Mol. Biol. Rev. 2012, 76, 16−32.

(10) Quail, D. F.; Joyce, J. A. Microenvironmental Regulation ofTumor Progression and Metastasis. Nat. Med. 2013, 19, 1423−1437.

(11) Rosenberg, S. A.; Restifo, N. P.; Yang, J. C.; Morgan, R. A.;Dudley, M. E. Adoptive Cell Transfer: a Clinical Path to EffectiveCancer Immunotherapy. Nat. Rev. Cancer 2008, 8, 299−308.

(12) Hontscha, C.; Borck, Y.; Zhou, H.; Messmer, D.; Schmidt□Wolf, I. G. Clinical Trials on CIK Cells: First Report of theInternational Registry on CIK Cells (IRCC). J. Cancer Res. Clin. Oncol. 2011, 137, 305−310.

(13) Kershaw, M. H.; Westwood, J. A.; Darcy, P. K. Gene□engineered T Cells for CancerTherapy. Nat. Rev. Cancer 2013, 13,525−541.

(14) Vivier, E.; Ugolini, S.; Blaise, D.; Chabannon, C.; Brossay, L.Targeting Natural Killer Cells and Natural Killer T Cells in Cancer.Nat. Rev. Immunol. 2012, 12, 239−252.

(15) Koehl, U.; Kalberer, C.; Spanholtz, J.; Lee, D. A.; Miller, J. S.;Cooley, S.; Lowdell, M.; Uharek, L.; Klingemann, H.; Curti, A.;Leung, W.; Alici, E. Advances in Clinical NK Cell

Studies: DonorSelection, Manufacturing and Quality Control. Oncoimmunology 2016,5, No. e1115178.
(16) Dianat-Moghadam, H.; Rokni, M.; Marofi, F.; Panahi, Y.;Yousefi, M. Natural Killer Cell-based Immunotherapy: FromTransplantation Toward Targeting Cancer Stem Cells. J. Cell. Physiol.2019, 234, 259−273.
(17) Suen, W. C.; Lee, W. Y.; Leung, K. T.; Pan, X. H.; Li, G.Natural Killer Cell-Based Cancer Immunotherapy: A Review on 10Years Completed Clinical Trials. Cancer Invest. 2018, 36, 431−457.
(18) Wang, K.; Han, Y.; Cho, W. C.; Zhu, H. The Rise of HumanStem Cell-derived Natural Killer Cells for Cancer Immunotherapy.Expert Opin. Biol. Ther. 2019, 19, 141−148.
(19) Johnson, L. A.; Morgan, R. A.; Dudley, M. E.; Cassard, L.;Yang, J. C.; Hughes, M. S.; Kammula, U. S.; Royal, R. E.; Sherry, R.M.; Wunderlich, J. R.; Lee, C. C.; Restifo, N. P.; Schwarz, S. L.;Cogdill, A. P.; Bishop, R. J.; Kim, H.; Brewer, C. C.; Rudy, S. F.;VanWaes, C.; Davis, J. L.; Mathur, A.; Ripley, R. T.; Nathan, D. A.Laurencot, C. M.; Rosenberg, S. A. Gene Therapy with Human andMouse T-cell Receptors Mediates Cancer Regression and TargetsNormal Tissues Expressing Cognate Antigen. Blood 2009, 114, 535−546.
(20) Lamers, C. H.; Sleijfer, S.; van Steenbergen, S.; van Elzakker, P.;van Krimpen, B.; Groot, C.; Vulto, A.; den Bakker, M.; Oosterwijk, E.;Debets, R.; Gratama, J. W. Treatment of Metastatic Renal CellCarcinoma with CAIX CAR-engineered T Cells: Clinical Evaluationand Management of On-target Toxicity. Mol. Ther. 2013, 21, 904−912.
(21) Morgan, R. A.; Yang, J. C.; Kitano, M.; Dudley, M. E.;Laurencot, C. M.; Rosenberg, S. A. Case Report of a Derious AdverseEvent Following the Administration of T Cells Transduced with aChimeric Antigen Receptor Recognizing ERBB2. Mol. Ther. 2010, 18,843−851.
(22) Parkhurst, M. R.; Yang, J. C.; Langan, R. C.; Dudley, M. E.;Nathan, D. A.; Feldman, S. A.; Davis, J. L.; Morgan, R. A.; Merino, M.J.; Sherry, R. M.; Hughes, M. S.; Kammula, U. S.; Phan, G. Q.; Lim, R.M.; Wank, S. A.; Restifo, N. P.; Robbins, P. F.; Laurencot, C. M.;Rosenberg, S. A. T. Cells Targeting Carcinoembryonic Antigen CanMediate Regression of Metastatic Colorectal Cancer but InduceSevere Transient Colitis. Mol. Ther. 2011, 19, 620−626.
(23) Zhang, J.; Niu, C.; Ye, L.; Huang, H.; He, X.; Tong, W. G.;Ross, J.; Haug, J.; Johnson, T.; Feng, J. Q.; Harris, S.; Wiedemann, L.M.; Mishina, Y.; Li, L. Identification of the Haematopoietic Stem CellNiche and Control of the Niche Size. Nature 2003, 425, 836−841.
(24) Shang, L.; Cheng, Y.; Zhao, Y. Emerging Droplet Microfluidics.Chem. Rev. 2017, 117, 7964−8040.
(25) Wang, H.; Zhao, Z.; Liu, Y.; Shao, C.; Bian, F.; Zhao, Y.Biomimetic Enzyme Cascade Reaction System in MicrofluidicElectrospray Microcapsules. Scie. Adv. 2018, 4, No. aat2816.
(26) Yu, Y.; Shang, L.; Gao, W.; Zhao, Z.; Wang, H.; Zhao, Y.Microfluidic Lithography of Bioinspired Helical Micromotors. Angew.Chem., Int. Ed. 2017, 56, 12127−12131.
(27) Zhu, P.; Wang, L. Passive and Active Droplet Generation withMicrofluidics: a Review. Lab on a Chip 2017, 17, 34−75.
(28) Fu, F.; Shang, L.; Zheng, F.; Chen, Z.; Wang, H.; Wang, J.; Gu,Z.; Zhao, Y. Cells Cultured on Core-Shell Photonic Crystal Barcodesfor Drug Screening. ACS Appl. Mater. Interfaces 2016, 8, 13840−13848.
(29) Jiang, W.; Li, M.; Chen, Z.; Leong, K. W. Cell-ladenMicrofluidic Microgels for Tissue Regeneration. Lab on a Chip2016, 16, 4482−4506.

(30) Li, F.; Truong, V. X.; Thissen, H.; Frith, J. E.; Forsythe, J. S.Microfluidic Encapsulation of Human Mesenchymal Stem Cells forArticular Cartilage Tissue Regeneration. ACS Appl. Mater. Interfaces2017, 9, 8589−8601.
(31) Wang, J.; Chen, G.; Zhao, Z.; Sun, L.; Zou, M.; Ren, J.; Zhao,Y. Responsive Graphene Oxide Gydrogel Microcarriers for Control□lable Cell Capture and Release. Sci. China Mater.2018, 61, 1314−1324.
(32) Yu, Y.; Shang, L.; Guo, J.; Wang, J.; Zhao, Y. Design ofCapillary Microfluidics for Spinning Cell-laden Microfibers. Nat.Protoc. 2018, 13, 2557−2579.
(33) Zhang, L.; Chen, K.; Zhang, H.; Pang, B.; Choi, C.-H.; Mao, A.S.; Liao, H.; Utech, S.; Mooney, D. J.; Wang, H.; Weitz, D. A.Microfluidic Templated Multicompartment Microgels for 3DEncapsulation and Pairing of Single Cells. Small 2018, 14,No. 1702955.
(34) Zhao, X.; Liu, S.; Yildirimer, L.; Zhao, H.; Ding, R.; Wang, H.;Cui, W.; Weitz, D. Injectable Stem Cell-Laden PhotocrosslinkableMicrospheres Fabricated Using Microfluidics for Rapid Generation ofOsteogenic Tissue Constructs. Adv. Funct. Mater. 2016, 26, 2809−2819.